T.V. Ahangama*

Dept. of Electrical and Electronic Engineering

University of Peradeniya

Sri Lanka

thushanthyaa@gmail.com

https://orcid.org/0009-0001-3770-8315

G.M.K.G.G.B. Gurunayake*

Dept. of Electrical and Electronic Engineering

University of Peradeniya

Sri Lanka

gihangurunayaka@gmail.com

https://orcid.org/0009-0003-2806-6239

I.A. Yalpathwala

Dept. of Electrical and Electronic Engineering

University of Peradeniya

Sri Lanka

isurianu96@gmail.com

J.V. Wijayakulasooriya

Dept. of Electrical and Electronic Engineering

University of Peradeniya

Sri Lanka

jan@eng.pdn.ac.lk

T.L. Dassanayake

Department of Physiology

Faculty of Medicine

University of Peradeniya

Sri Lanka

tharaka.dassanayake@med.pdn.ac.lk

N. Harischandra

Dept. of Electrical and Electronic Engineering

University of Peradeniya

Sri Lanka

nalin@ee.pdn.ac.lk

Kwangtaek Kim

Dept. of Computer Science

Kent State University

United States

kkim@cs.kent.edu

R.D.B. Ranaweera

Dept. of Electrical and Electronic Engineering

University of Peradeniya

Sri Lanka

ruwan@eng.pdn.ac.lk

NOTE: This preprint reports new research that has not been certified by peer review and should not be used to guide clinical practice.

*These authors contributed equally to this work.

Title: EEG-Based Frequency Domain Separation of Upward and Downward Movements of the Upper Limb.

Running title: EEG-based same joint movement classification.

ABSTRACT

One of the fundamental challenges encountered when implementing the Motor Imagery based Brain-Computer Interfacing (BCI) paradigm is accurately classifying the Electroencephalography (EEG) signals that originate due to the same joint movements. This emanates from the limited spatial proximity in the corresponding brain regions. Here, we explore the feasibility of distinguishing arm-reaching movements specific to the right hand using multiple frequency bands in EEG signals despite the limited spatial differentiation of induced potentials. To address this challenge, a channel averaging method was used combining six electrodes positioned in close proximity to the motor cortex, intending to isolate and enhance electromagnetic activity in the brain associated with arm movements. This study was further refined by focusing on two distinct frequency bands: mu (8-12Hz) and beta (12-30Hz), each associated with different cognitive and motor functions. The results of our study revealed promising outcomes across two classification methods. Utilizing the Support Vector Machine (SVM) classification method, our proposed approach achieved an average accuracy of 59.3% while the K-Nearest Neighbors (KNN) classification approach yielded an average accuracy of 61.63% in distinguishing between upward and downward movements of the right arm.

Keywords: BCI, Channel reduction, EEG, Motor movement, Same joint, Same limb.

INTRODUCTION

Brain-computer interfacing (BCI) is a technology that has the potential to both improve functions in healthy people and also restore usable function in people who are severely affected by a wide range of debilitating neuromuscular illnesses. The primary objective of BCI signal processing is to extract characteristics from obtained brain signals and convert them into logical control instructions for BCI applications [1]. Applications of brain-computer interfaces based on electroencephalography (EEG) that use motor movements and motor-imagery (MI) data have the potential to be revolutionary in the clinical and entertainment fields. They excel by not necessitating external stimuli, remaining cost-effective, and being entirely non-invasive. Moreover, the discrete movement intention paradigm which utilizes the EEG signals collected before movement onset can be directly used in motor rehabilitation and in navigating through the environment accordingly as it detects movement intention [2].

Most widely deployed left and right upper limb or upper and lower limb movements serve as the basis for motor imagery-based control systems. Numerous research studies have shown improved accuracy in classifying different limb motions [3]–[7] since the motor cortex has unique, spatially separable regions that correspond to specific areas of the human body. Thus, event-related desynchronization (ERD) or event-related synchronization (ERS) induced in corresponding areas can be recognized by algorithms that identify distinct spatial patterns of activity [8], [9].

The classification of EEG signals that correspond to the same limb is more challenging than that of separate limbs because the EEG signals that correspond to the same limb movements originate in adjacent areas in the motor cortex with minimal spatial separation. Several studies have shown that brain activity captured by EEG can be used to decode motor intents associated with the same limb activities such as reaching, grasping, finger movements, and complex limb movements

[10]–[15]. However, it is challenging to separate the EEG signals induced due to distinct movements done by the same joint, as the differences among spatial activations get even smaller [16]. Besides the potentials originating from the primary motor cortex, these joint movements may be correlated with the potentials that originate from locations such as the premotor cortex and the supplementary motor cortex as well [17]. Furthermore, the EEG rhythms that can discriminate joint movements can be modulated not only within the intended movement time segment but also within the segment that correlates with the movement intention that occurs before movement onset [14], [18]. Therefore, in contrast to spatial separation, it is essential to focus more on identifying unique features of the EEG signals triggered by different motor movements carried out by the same joint.

In the EEG signal analysis pipeline, classification methods play a pivotal role since higher accuracy enables the bearer to execute precise motor controls of fine movements with high reliability. Traditional machine learning (ML) techniques such as SVM, Linear Discriminant Analysis (LDA), and Logistic Regression have dominated the literature as classification methods for Sensory Motor Rhythm (SMR) based BCI paradigms over Deep Learning methods [2].

This study examines the feasibility of using EEG signals induced due to upward and downward movements performed by the right upper limb, to distinguish them in the frequency domain. The analysis involved combining the EEG signals collected from the electrodes positioned in brain regions that are closely associated with motor planning and execution, considering time segments, both before and after the movement onset. Although the analysis pipeline is done in offline mode in this study, the computational simplicity of the suggested model serves the purpose of being feasible for real-time implementation.

MATERIALS AND METHODS

Data Acquisition and Description

The EEG data for this study was sourced from the "Multimodal signal dataset for 11 intuitive movement tasks from single upper extremity during multiple recording sessions" [19]. This dataset includes 60-channel EEG, 7-channel electromyography (EMG), and 4-channel electro-oculography (EOG) signals recorded at 2500Hz across three days. It was gathered from 25 healthy right-handed subjects and notch filtered at 60Hz to reduce external electrical noise. Electrode positioning followed the international standard 10-20 system. The experiment involved upper extremity actions, including arm-reaching in six directions, hand-grasping of three objects, and wrist-twisting with two motions performed by the right hand. [19]

Experimental Paradigm

Figure 1 illustrates the timing diagram for both real and motor imagery tasks. The experiment was initiated with a 4-second resting stage, after a gray background and a black cross displayed on the monitor. Subsequently, participants were presented with textual task instructions serving as visual cues for 3 seconds. Following this, participants received a visual cue indicating whether to execute a motor activity or engage in motor imagery within a 4-second timeframe. [19]

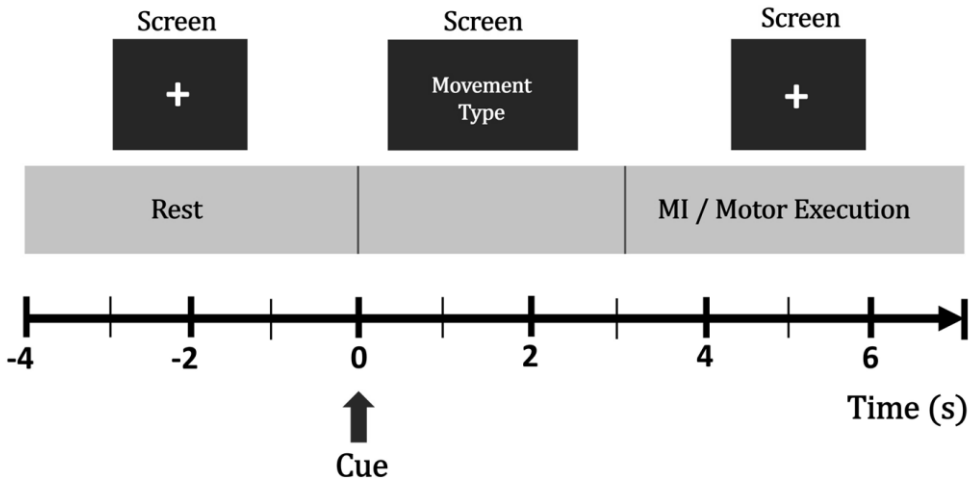

Figure 1. The timing diagram of the experiment

Dataset Preparation

In the original dataset, each subject performed 50 movements from each type of arm reaching real movements randomly. Corresponding EEG (60 channels), EMG (8 channels), and EOG (4 channels) data were recorded simultaneously for all 300 movement epochs. Out of them, data from the EEG channels were selected and subjected to bandpass FIR filtering (0.5-100 Hz) to eliminate high-frequency noise and drifts in all real-reaching movements. Since this study explores only the upward and downward movements, the epochs corresponding to these movements were segregated from all the recorded reaching real movements considering the given trigger points. This separation was done in such a way that each subject had 100 epochs, with 50 epochs per movement type.

Signal Pre-Processing

EEG functions by measuring the integration of all postsynaptic potentials of the populations of neurons over the scalp and has a lower spatial resolution compared to functional Magnetic Resonance Imaging (fMRI), Electrocorticogram (ECoG), etc. Therefore, EEG data are contaminated with artifacts including ECG, eye movements, voluntary muscle activity, and noise from surrounding electronic equipment [20]. Hence following preprocessing was done on the data set to remove these noise artifacts to improve the SNR.

All the data were resampled at 500 Hz and the artifactual epochs were removed by visual inspection considering the extreme values and abnormal trends. It was verified by visual inspection that no noisy and corrupted channels were present, and then the data were re-referenced with Common Average Referencing (CAR) [21] as stated in equation 1 to reduce the background noise.

$$y_{CAR}(c,n) = y(c,n) - \frac{1}{N}\sum_{i=1}^{N} y(i,n) \quad \ldots(1)$$

where $y_{CAR}(c,n)$ denotes the common averaged potential at channel c and sample point n which was calculated by subtracting the average potential of total N channels at that sample point from EEG potential $y(c,n)$ at channel c and sample point n.

Subsequently, Independent Component Analysis (ICA) (Potter et al., 2002; Xue et al., 2006) was performed using the Infomax algorithm as it has shown better performance in isolating artifacts [24]. After inspecting the spatial topography, temporal variation, and power spectral density of the isolated components, a few artifacts were chosen to be removed, so that the information loss is minimal while increasing the SNR. Typically, two Independent Components that contain eye blink artifacts as shown in Figure 2 were selected per subject because eye blinks are typically 10 times larger in amplitude compared to ongoing EEG signals as depicted in Figure 3 which has a huge impact on the preferred data. Finally, the average baseline from -500 ms to 0 ms with respect to cue was subtracted as the final stage of the pre-processing.

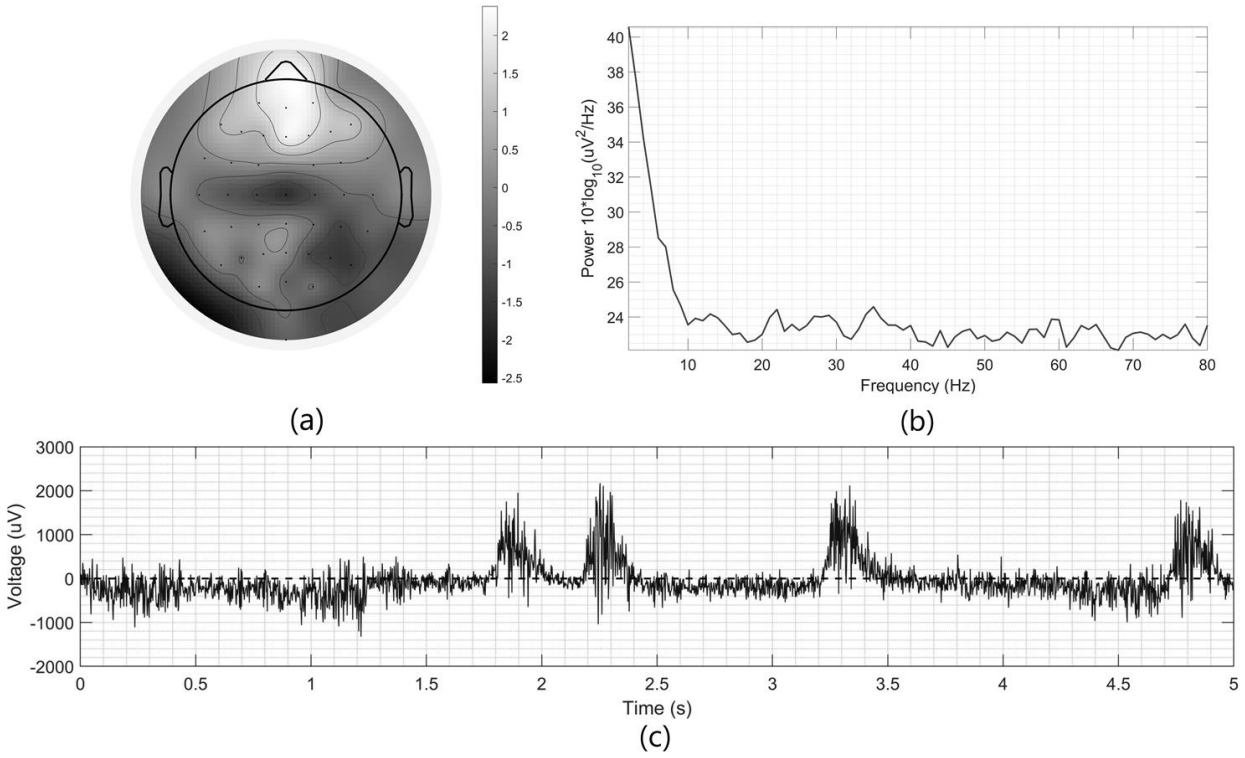

Figure 2. Characteristics of an eye blink artifact which was isolated and removed using infomax-ICA. (a) shows the spatial activation topography, (b) shows power spectral density, and (c) shows representation in the time domain.

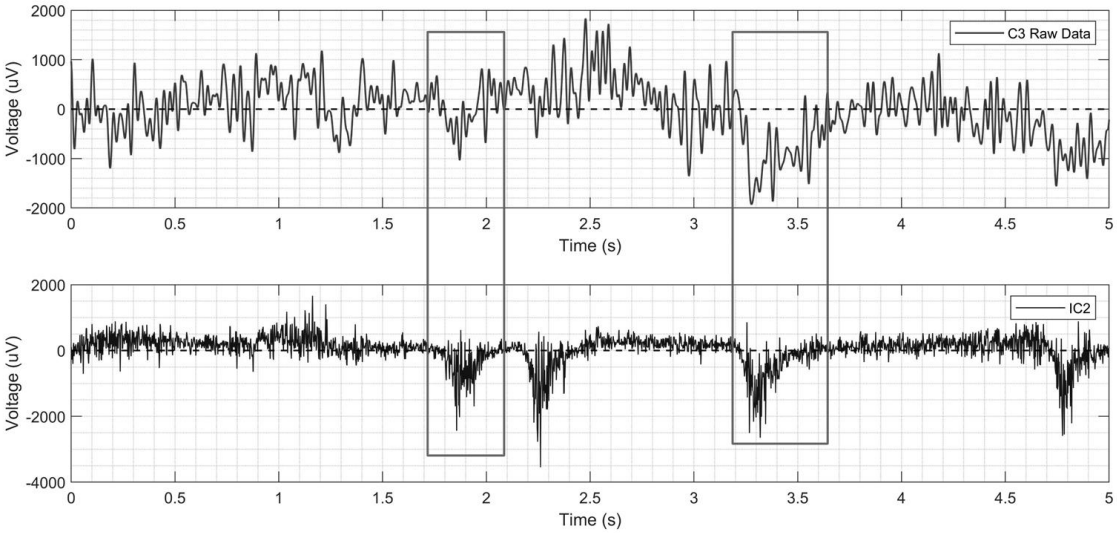

Figure 3. Time domain representation of the presence of the eye blink artifact (IC2) within the raw data of C3, showcasing their shared characteristics.

Channel Selection

Electrode positioning in the 10-20 system corresponds to different brain regions and, the EEG signals obtained from each electrode represent activity in different brain areas. This research was conducted by extracting the frequency domain features from the EEG signals acquired from a set of selected electrodes, based on the spatial correspondence of the brain and muscles [25]. Considering the high probability of capturing electromagnetic activity which is correlated with the motor cortex that controls the muscles in the right upper limb [26], we selected FC5, FC3, FC1, C5, C3, and C1 electrodes as shown in Figure 4.

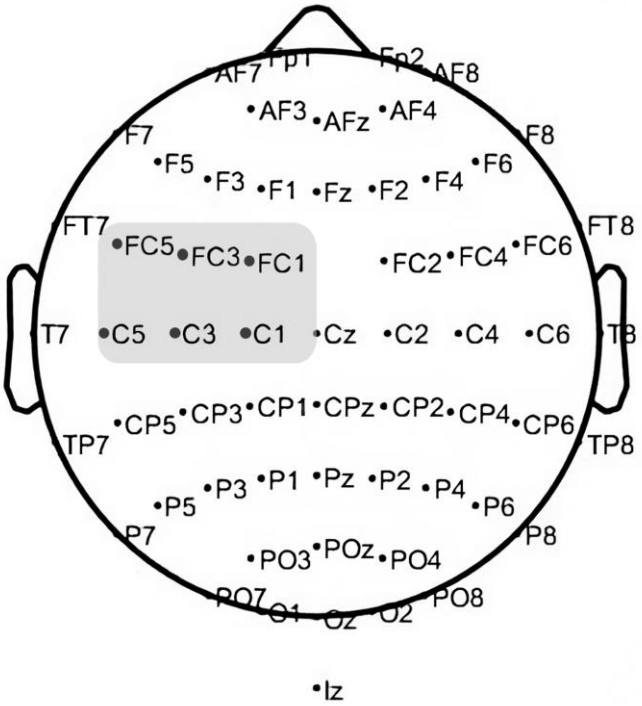

Figure 4. Selected 6 electrodes for the channel averaging method.

The C1, C3, and C5 channels were selected because they are located over the arm area of the motor homunculus of the left primary motor cortex, which is primarily responsible for right-side motor control [27]. FC1, FC3, and FC5 channels were selected as they were placed covering the left half of the pre-motor and the supplementary motor cortices. The supplementary motor cortex is mainly involved with motor planning whereas the pre-motor cortex is responsible for carrying out movement, sequences of movements, and the selection of movements based on sensory information [27]. As the next step in our approach, a single signal was derived by averaging each of the epochs over the selected channels, to consolidate the effects of all the signals that were highly correlated with motor movements. We expected the noise and brain signals outside the relevant brain area to get reduced while the signal from the relevant area remained by this technique.

Feature Extraction

The spontaneous EEG recordings, also known as spontaneous electrical activity, have distinct waveforms that predominate over a wide range of frequencies. Scientifically, there are five frequency

bands of spontaneous EEG activity. Each of these frequency bands has a rhythmic activity that is characterized by a specific scalp distribution and biological importance [28].

The Mu (8-12 Hz) and the Beta (13-30 Hz) Sensory-Motor Rhythms (SMR) have proved to undergo modulations whenever there is a movement of a large body part which are most prominent in EEG signals acquired from C3 and C4 electrodes [29]. This is a phenomenon known as Event-related synchronization (ERS) and Event-Related Desynchronization (ERD) which occur during movement and relaxation respectively. These ERDs and ERSs which lead to short-lasting and circumscribed attenuation of mu and beta rhythms have played an essential role in implementing reliable EEG-based BCI systems across the past three decades. Despite SMR bands not containing kinematic parameter information which has been confirmed by several studies [30], [31], they have been used to distinguish among different motor movements and they provide a reliable feature for BCI. Modulation of such EEG rhythms correlates with motor planning, motor movement, and motor imagery which can be used to classify brain states that relate to planning or imagination of different types of limb movements [32].

In this study, extracting the band-pass signal in the frequencies ranging between 8-12 Hz (Mu), 12-30 Hz (Beta), and 8-30 Hz (Both Mu and Beta) from the wideband signal was performed using an FIR filter which has a linear phase response. Before calculating the band power, part of the signal was selected from -0.5 to 2.5 s from the given timing paradigm (Figure 1), considering the ERP over the selected epochs of the averaged signal.

The Welch's Power Spectral Density (PSD) was calculated for each averaged signal with a window length of 1000 sample points (2s) with an overlapping of 500 sample points (1s). PSD values within each band of each epoch were considered as the features. The extraction of spectral features involved several steps as follows (equations 2, 3, and 4).

$$p_c(f,s) = \frac{1}{W}\sum_{n=-\frac{w}{2}}^{\frac{w}{2}-1} \left| y_{CAR}\left(c, n+\frac{w}{2}+1, s\right) \cdot H(n) \cdot \exp\left(j\frac{2\pi}{w}fn\right)\right|^2 \quad \ldots(2)$$

$$H(n) = \frac{1+\cos\left(\frac{2\pi n}{W}\right)}{2} \quad \ldots(3)$$

Where $p_c(f,s)$ denotes the PSD at channel c and frequency f for segment s. $H(n)$ is the Hanning window of window length W set as 1000 sample points. PSD for each trial was normalized by,

$$P_C(f,s) = \log\left(\frac{p_c(f,s)}{\frac{1}{M}\sum_{s=1}^{M} p_c(f,s)}\right) \quad \ldots(4)$$

Where $P_C(f,s)$ is the normalized PSD of each segment with symbols f, c, s, and M denoting frequency, channel number, segment, and the total number of segments.

Feature Classification

The data were randomly split into training and testing sets constituting 70% and 30% of the data collected respectively. Training data consisted of 35 trials since each subject had 50 epochs for each movement, whereas the remaining epochs were considered as the testing data. Subjects containing less than 35 epochs from either up or down movements after the removal of bad trials were neglected. MATLAB [33] classification learner Toolbox was used to run automated hyperparameter optimization using Bayesian optimization, which yielded SVM and KNN as the best-performing algorithms for the extracted features. The validation results were obtained by feeding the 70 training epochs (35 epochs for each movement type) to the classification learner with a K-fold value of 5. The classification accuracy was evaluated using the Geometric mean (G mean) of the sensitivity and specificity of the classifiers (equations 5, 6, and 7).

$$Gmean = \sqrt{Sensitivity \times Specificity} \quad \ldots(5)$$

Where,

$$Sensitivity = \frac{TPR}{TPR+FNR} \quad \ldots(6)$$

And,

$$Specificity = \frac{TNR}{TNR+FPR} \quad \ldots(7)$$

RESULTS

In the proposed method, three different frequency bands from the measured wideband EEG signals were extracted, intending to identify a particular feature in the frequency domain, that corresponded to upward and downward movements of the upper limb, and two different classifiers were used to differentiate the extracted features. According to the mean confusion matrices obtained by the proposed method, as depicted in Figure 5 and Figure 6, both upward and downward movements were classified with an average accuracy of 60% without getting biased for any of the movement types.

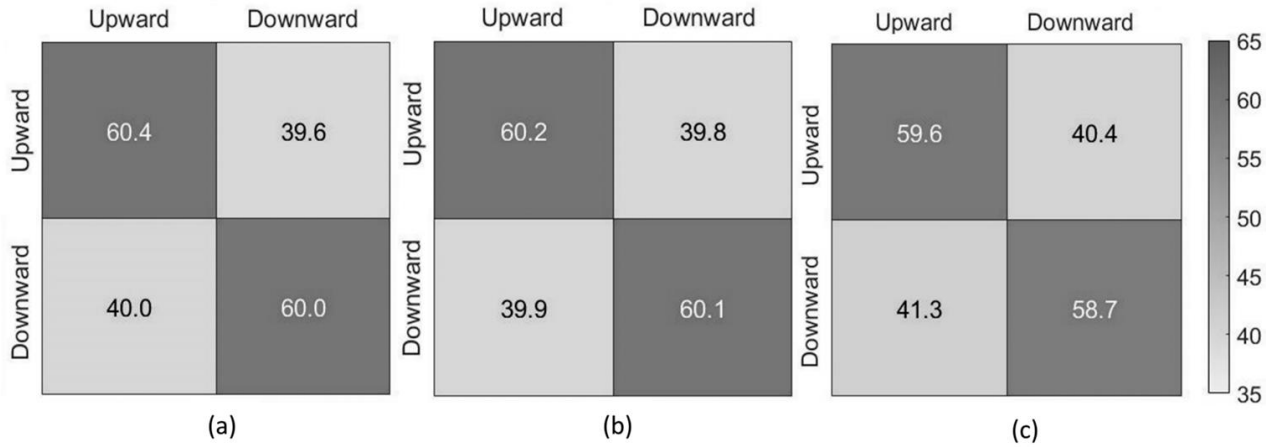

Figure 5. The mean confusion matrices (%) obtained from the SVM classifier. (a) corresponded to the 8-12Hz (b) corresponded to the 12-30Hz (c) corresponded to the 8-30Hz.

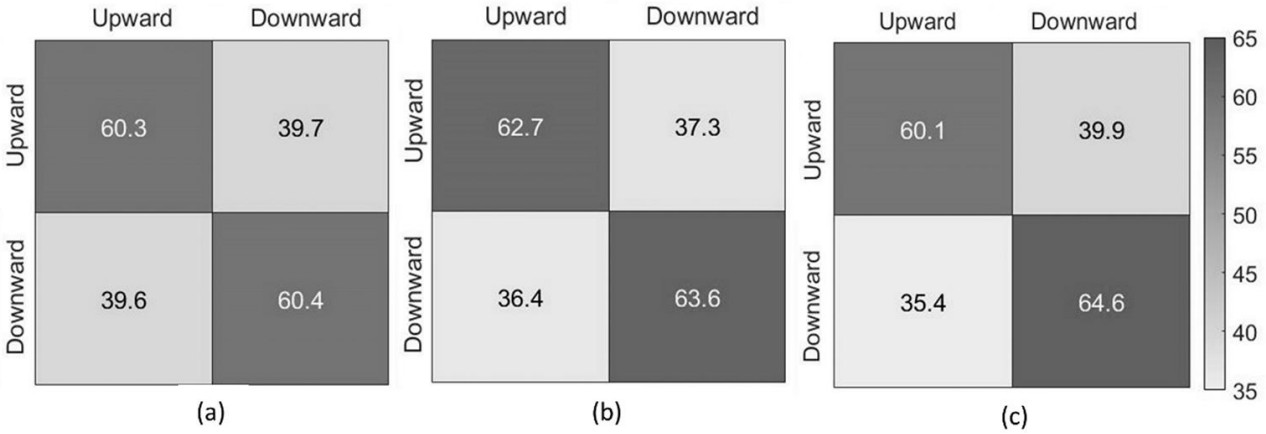

Figure 6. The mean confusion matrices (%) obtained from the KNN classifier. (a) corresponded to the 8-12Hz (b) corresponded to the 12-30Hz (c) corresponded to the 8-30Hz.

Figure 7 depicts the histograms for both SVM and KNN classifiers, for each selected frequency band, using the G-mean values obtained for each of the selected subjects. The highest classification accuracy for a single subject was 76% from SVM and 74% from KNN classifiers utilizing the 8-12 Hz band.

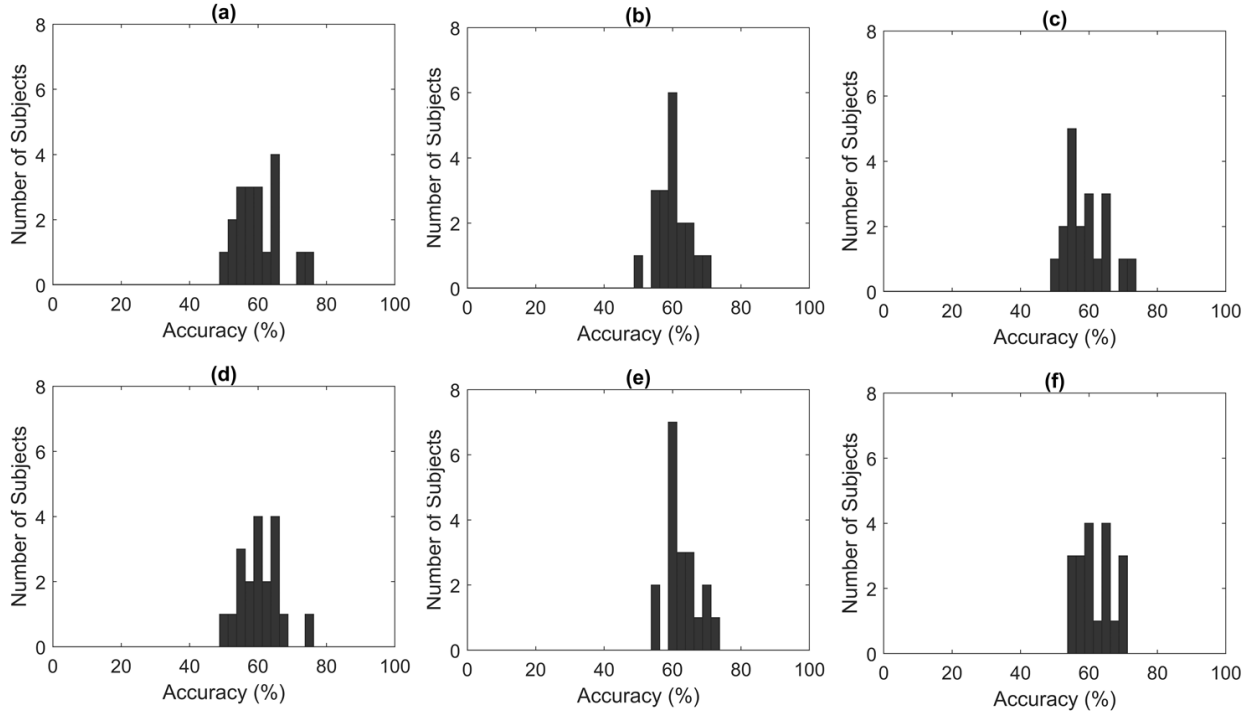

Figure 7. Distribution of accuracies across selected classification methods and SMR bands. Subfigures show the performance of SVM classifiers in (a) Mu, (b) Beta, and (c) Mu and Beta bands, as well as KNN classifiers in (d) Mu, (e) Beta, and (f) Mu and Beta.

Based on the results in Table 1, both the SVM and KNN classification techniques demonstrate average accuracies of approximately 60 ± 1.5% across all three frequency bands significantly outperforming a random chance (p-value < 0.00005). Figure 8 summarizes the performance of selected classifiers on the data.

Table 1. Overall results of SVM and KNN classifiers across the selected frequency bands. Indicated p-values are for the obtained accuracies with each method compared to a random chance of 0.5.

	SVM			KNN		
	8-12Hz	12-30Hz	8-30Hz	8-12Hz	12-30Hz	8-30Hz
μ	0.60	0.60	0.59	0.60	0.63	0.62
$\pm\sigma$	0.065	0.044	0.059	0.056	0.047	0.053
p-Value ($\times 10^{-5}$)	0.435	0.006	0.288	0.048	0.0001	0.002

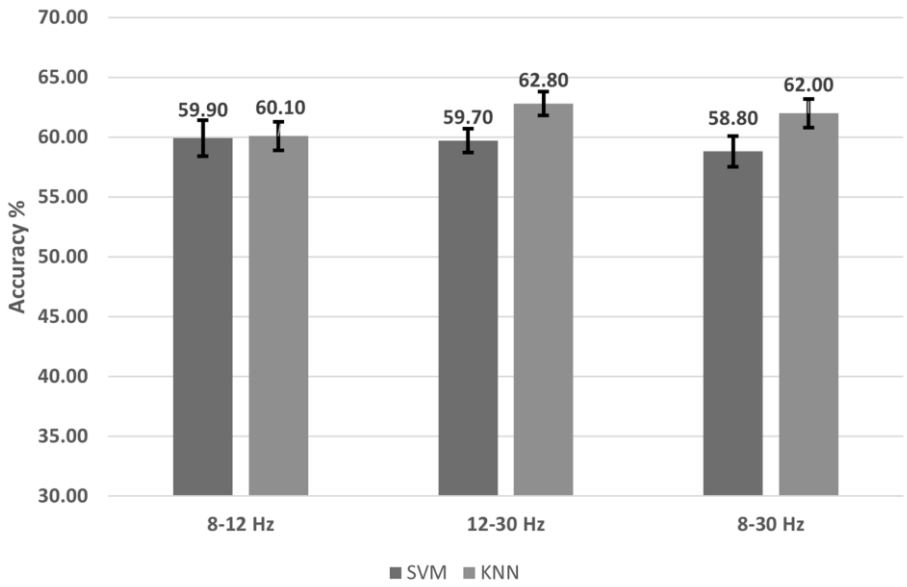

Figure 8. Classification accuracy comparison by both SVM and KNN classifiers.

DISCUSSION

Considering the separation of the same limb movements in recent studies, five different complex activities executed by the same limb which activates different regions of the brain were differentiated with an average classification accuracy of 94.0 ± 2.7% by Mohseni et al.[14]. However, when the movement types become similar to each other the discrimination becomes difficult as the activation regions draw closer among movements. Xu et al. have obtained about 60% and 40% accuracy in 2-class and 3-class classifications respectively using EEG signals that occurred due to MI-hand, MI-forearm, MI-arm, and rest with 4 different sets of electrodes [34] while Ma et al. have separated

imagery movement of the right hand, right elbow, vs resting with eyes open at an average accuracy of 68.68 ± 2.44% [35]. It is worth mentioning that in some research studies, the reported overall accuracy for multiclass movement classification includes the "rest" category. As a result, the accuracy tends to be higher because distinguishing between movement and rest is generally done with greater accuracy. Several seminal studies have confirmed that kinematic parameters of motor movements (e.g., position, velocity) are embedded in SMR bands below 2Hz [30], [36], [37]. Using time domain features in low-frequency EEG Ofner et al. have achieved accuracies of 55% (movement vs. movement), 87% (movement vs. rest) for executed movements, and 27% (movement vs. movement), 73% (movement vs. rest) for imaginary movements, elbow flexion, elbow extension, forearm supination, forearm pronation, hand close, and hand open [38]. However, decoding accuracies of kinematic information from low-frequency SMR bands have been reported to be poor [39] and, the average accuracies of 46.8% in the 5-class scenario and 53.4% in the 4-class scenario obtained from Ma et al. for four different joints and the resting state, using time distributed attention networks show that information within alpha and beta frequency ranges in MI task perform better [40]. Achanccaray & Hayashibe et al. have achieved maximum mean accuracies of 78.46 ± 12.50% and 76.72 ± 11.67% for two (flexion/extension) and three (flexion/extension/grasping) class MI tasks respectively using deep learning algorithms [12]. Further, it is evident through results that movements involving different joints are better distinguishable than movements involving the same joints [38]. However, an effective approach in extracting features that yields satisfactory accuracies for discriminating movements about the same joints remains elusive in current research to the best of our knowledge.

In comparison to state-of-the-art, the findings of our study reveal that it is possible to distinguish similar joint movements by analyzing the power spectral density of both the alpha and beta bands with reduced computational complexity. The reduction of the number of electrodes to 6 channels that relate to primary motor, premotor, and supplementary motor cortices, also improves the reliability

and reduces the required computational power of the EEG acquisition. Furthermore, when utilizing electrodes that cover the entire head to extract features, the analysis encompasses information from the entire brain, including responses to external stimuli like visual or auditory instructions. In such cases, movements might be classified based on potentials induced by these external factors. In contrast, our method concentrates solely on electrodes centered around the motor cortex, the potentials involved with the analysis have a high probability of containing motor movement-related information.

The following limitations of our study can be identified. Due to subject variability, each subject has to be trained separately which takes a significant time to train. Although artifactual epochs can be removed in offline analysis by visual inspection, a real-time BCI system operates under the constraint of processing these potentially problematic epochs in real-time conditions. Further, Preprocessing filter kernels were non-causal to avoid time delays, but a real-time application must employ causal kernels which adds a delay.

Further studies need to explore the effect of the selected electrodes and the use of time-frequency features for classification performance. As the new evidence suggests it may not be that important to remove artifacts, and in some cases, it can actually be detrimental due to the loss of statistical power [41]. Therefore, the impact of the exclusion of preprocessing needs to be explored considering the importance of implementing a cost-effective real-time BCI.

CONCLUSION

The lower spatial separation makes it challenging to classify EEG signals induced due to the same joint movements. Therefore, this study was carried out with the intention of detecting unique features in the frequency domain directly correlated with the same joint motor activities.

During the feature extraction process, the EEG signals induced by up and down right-hand movements recorded by the electrodes corresponding to brain cortices, significantly correlated with motor movement activities were averaged. Subsequently, two different frequency bands (mu and beta) and both together were isolated from the averaged signal to explore the impact of Welch's PSD values on the EEG signals. In the classification process, we employed SVM and KNN methods to achieve robust results.

Our findings reveal promising insights into the potential effectiveness of frequency domain features in EEG signals for distinguishing the same joint movements by using a computationally simple and pragmatic model. This study contributes valuable knowledge to the field of EEG signal analysis and may pave the way for enhanced understanding and practical applications in Brain-Computer Interfacing (BCI) research.

Conflict of interest statement

The authors declare that they have no competing interests.

Data availability statement

The data that support the findings of this study are openly available in the GigaDB repository, at http://dx.doi.org/10.5524/100788.

REFERENCES

[1] B. He, Ed., *Neural Engineering*. Cham: Springer International Publishing, 2020. doi: 10.1007/978-3-030-43395-6.

[2] R. Abiri, S. Borhani, E. W. Sellers, Y. Jiang, and X. Zhao, "A comprehensive review of EEG-based brainâ€"computer interface paradigms," *J Neural Eng*, vol. 16, no. 1, p. 11001, Jan. 2019, doi: 10.1088/1741-2552/aaf12e.

[3] S. Bhattacharyya, A. Khasnobish, S. Chatterjee, A. Konar, and D. N. Tibarewala, "Performance analysis of LDA, QDA and KNN algorithms in left-right limb movement

classification from EEG data," in *2010 International Conference on Systems in Medicine and Biology*, 2010, pp. 126–131. doi: 10.1109/ICSMB.2010.5735358.

[4] K. Lafleur, K. Cassady, A. Doud, K. Shades, E. Rogin, and B. He, "Quadcopter control in three-dimensional space using a noninvasive motor imagery-based brain-computer interface," *J Neural Eng*, vol. 10, no. 4, Aug. 2013, doi: 10.1088/1741-2560/10/4/046003.

[5] T. Li, J. Hong, J. Zhang, and F. Guo, "Brain-machine interface control of a manipulator using small-world neural network and shared control strategy," *J Neurosci Methods*, vol. 224, pp. 26–38, Mar. 2014, doi: 10.1016/j.jneumeth.2013.11.015.

[6] X. Lun, J. Liu, Y. Zhang, Z. Hao, and Y. Hou, "A Motor Imagery Signals Classification Method via the Difference of EEG Signals Between Left and Right Hemispheric Electrodes," *Front Neurosci*, vol. 16, May 2022, doi: 10.3389/fnins.2022.865594.

[7] G. Prapas, K. Glavas, K. D. Tzimourta, A. T. Tzallas, and M. G. Tsipouras, "Mind the Move: Developing a Brain-Computer Interface Game with Left-Right Motor Imagery," *Information*, vol. 14, no. 7, p. 354, Jun. 2023, doi: 10.3390/info14070354.

[8] H. Ramoser, J. Muller-Gerking, and G. Pfurtscheller, "Optimal spatial filtering of single trial EEG during imagined hand movement," *IEEE Transactions on Rehabilitation Engineering*, vol. 8, no. 4, pp. 441–446, 2000, doi: 10.1109/86.895946.

[9] Y. Wang, S. Gao, and X. Gao, "Common Spatial Pattern Method for Channel Selelction in Motor Imagery Based Brain-computer Interface," in *2005 IEEE Engineering in Medicine and Biology 27th Annual Conference*, 2005, pp. 5392–5395. doi: 10.1109/IEMBS.2005.1615701.

[10] F. Shiman *et al.*, "Classification of different reaching movements from the same limb using EEG," *J Neural Eng*, vol. 14, no. 4, p. 46018, Jun. 2017, doi: 10.1088/1741-2552/aa70d2.

[11] C. Yong Xinyi AND Menon, "EEG Classification of Different Imaginary Movements within the Same Limb," *PLoS One*, vol. 10, no. 4, pp. 1–24, Aug. 2015, doi: 10.1371/journal.pone.0121896.

[12] D. Achanccaray and M. Hayashibe, "Decoding hand motor imagery tasks within the same limb from eeg signals using deep learning," *IEEE Trans Med Robot Bionics*, vol. 2, no. 4, pp. 692–699, 2020.

[13] R. D. Ranaweera, T. M. Talavage, and A. Krishnan, "Time-frequency Features Differentiate Direction of Finger Movement in Cued and Self-paced Tasks," in *Conference Proceedings. 2nd International IEEE EMBS Conference on Neural Engineering, 2005.*, Mar. 2005, pp. 551–554. doi: 10.1109/CNE.2005.1419682.

[14] M. Mohseni, V. Shalchyan, M. Jochumsen, and I. K. Niazi, "Upper limb complex movements decoding from pre-movement EEG signals using wavelet common spatial patterns," *Comput. Methods Programs Biomed.*, vol. 183, no. 105076, p. 105076, Jan. 2020.

[15] M. Tavakolan, Z. Frehlick, X. Yong, and C. Menon, "Classifying three imaginary states of the same upper extremity using time-domain features," *PLoS One*, vol. 12, no. 3, pp. e0174161-, Mar. 2017, [Online]. Available: https://doi.org/10.1371/journal.pone.0174161

[16] R. Alazrai, H. Alwanni, and M. I. Daoud, "EEG-based BCI system for decoding finger movements within the same hand," *Neurosci Lett*, vol. 698, pp. 113–120, 2019, doi: https://doi.org/10.1016/j.neulet.2018.12.045.

[17] P. Ofner and G. R. Müller-Putz, "Using a noninvasive decoding method to classify rhythmic movement imaginations of the arm in two planes," *IEEE Trans Biomed Eng*, vol. 62, no. 3, pp. 972–981, 2014.

[18] O. Bai *et al.*, "Prediction of human voluntary movement before it occurs," *Clinical Neurophysiology*, vol. 122, no. 2, pp. 364–372, 2011, doi: https://doi.org/10.1016/j.clinph.2010.07.010.

[19] J.-H. Jeong *et al.*, "Multimodal signal dataset for 11 intuitive movement tasks from single upper extremity during multiple recording sessions," *Gigascience*, vol. 9, no. 10, Aug. 2020, doi: 10.1093/gigascience/giaa098.

[20] W. Peng, "EEG preprocessing and denoising," *EEG Signal Processing and Feature Extraction*, pp. 71–87, 2019.

[21] K. A. Ludwig, R. M. Miriani, N. B. Langhals, M. D. Joseph, D. J. Anderson, and D. R. Kipke, "Using a Common Average Reference to Improve Cortical Neuron Recordings From Microelectrode Arrays," *J Neurophysiol*, vol. 101, no. 3, pp. 1679–1689, 2009, doi: 10.1152/jn.90989.2008.

[22] M. Potter, N. Gadhok, and W. Kinsner, "Separation performance of ICA on simulated EEG and ECG signals contaminated by noise," in *IEEE CCECE2002. Canadian Conference on Electrical and Computer Engineering. Conference Proceedings (Cat. No.02CH37373)*, 2002, pp. 1099–1104 vol.2. doi: 10.1109/CCECE.2002.1013100.

[23] Z. Xue, J. Li, S. Li, and B. Wan, "Using ICA to Remove Eye Blink and Power Line Artifacts in EEG," in *First International Conference on Innovative Computing, Information and Control - Volume I (ICICIC'06)*, 2006, pp. 107–110. doi: 10.1109/ICICIC.2006.543.

[24] A. Delorme, T. Sejnowski, and S. Makeig, "Enhanced detection of artifacts in EEG data using higher-order statistics and independent component analysis," *Neuroimage*, vol. 34, no. 4, pp. 1443–1449, 2007.

[25] W. Schellekens, C. Bakker, N. F. Ramsey, and N. Petridou, "Moving in on human motor cortex. Characterizing the relationship between body parts with non-rigid population response fields," *PLoS Comput. Biol.*, vol. 18, no. 4, p. e1009955, Apr. 2022.

[26] C. L. Scrivener and A. T. Reader, "Variability of EEG electrode positions and their underlying brain regions: visualizing gel artifacts from a simultaneous EEG-fMRI dataset," *Brain Behav*, vol. 12, no. 2, p. e2476, 2022, doi: https://doi.org/10.1002/brb3.2476.

[27] H. Mushiake, M. Inase, and J. Tanji, "Neuronal activity in the primate premotor, supplementary, and precentral motor cortex during visually guided and internally determined sequential movements," *J. Neurophysiol.*, vol. 66, no. 3, pp. 705–718, Sep. 1991.

[28] S. Sanei and J. A. Chambers, *EEG signal processing*. John Wiley & Sons, 2013.

[29] G. Pfurtscheller and F. H. L. Da Silva, "Event-related EEG/MEG synchronization and desynchronization: basic principles," *Clinical neurophysiology*, vol. 110, no. 11, pp. 1842–1857, 1999.

[30] J.-H. Kim, F. Bießmann, and S.-W. Lee, "Decoding three-dimensional trajectory of executed and imagined arm movements from electroencephalogram signals," *IEEE Transactions on Neural Systems and Rehabilitation Engineering*, vol. 23, no. 5, pp. 867–876, 2014.

[31] A. Korik, R. Sosnik, N. Siddique, and D. Coyle, "Imagined 3D hand movement trajectory decoding from sensorimotor EEG rhythms," in *2016 IEEE International Conference on Systems, Man, and Cybernetics (SMC)*, 2016, pp. 4591–4596.

[32] C. Neuper and G. Pfurtscheller, "Event-related dynamics of cortical rhythms: frequency-specific features and functional correlates," *Int. J. Psychophysiol.*, vol. 43, no. 1, pp. 41–58, Dec. 2001.

[33] The MathWorks Inc., "MATLAB version: 9.10.0 (R2021a)." The MathWorks Inc., Natick, Massachusetts, United States, 2021. [Online]. Available: https://www.mathworks.com

[34] B. Xu *et al.*, "Phase Synchronization Information for Classifying Motor Imagery EEG From the Same Limb," *IEEE Access*, vol. 7, pp. 153842–153852, 2019, doi: 10.1109/ACCESS.2019.2948676.

[35] X. Ma, S. Qiu, and H. He, "Multi-channel EEG recording during motor imagery of different joints from the same limb," *Sci Data*, vol. 7, no. 1, p. 191, Jun. 2020, doi: 10.1038/s41597-020-0535-2.

[36] T. J. Bradberry, R. J. Gentili, and J. L. Contreras-Vidal, "Fast attainment of computer cursor control with noninvasively acquired brain signals," *J Neural Eng*, vol. 8, no. 3, p. 36010, 2011.

[37] T. J. Bradberry, R. J. Gentili, and J. L. Contreras-Vidal, "Reconstructing three-dimensional hand movements from noninvasive electroencephalographic signals," *Journal of neuroscience*, vol. 30, no. 9, pp. 3432–3437, 2010.

[38] P. Ofner, A. Schwarz, J. Pereira, and G. R. Müller-Putz, "Upper limb movements can be decoded from the time-domain of low-frequency EEG," *PLoS One*, vol. 12, no. 8, pp. e0182578-, Aug. 2017, [Online]. Available: https://doi.org/10.1371/journal.pone.0182578

[39] Y. Gu, K. Dremstrup, and D. Farina, "Single-trial discrimination of type and speed of wrist movements from EEG recordings," *Clinical neurophysiology*, vol. 120, no. 8, pp. 1596–1600, 2009.

[40] X. Ma, S. Qiu, and H. He, "Time-distributed attention network for EEG-based motor imagery decoding from the same limb," *IEEE Transactions on Neural Systems and Rehabilitation Engineering*, vol. 30, pp. 496–508, 2022.

[41] A. Delorme, "EEG is better left alone," *Sci Rep*, vol. 13, no. 1, p. 2372, Feb. 2023, doi: 10.1038/s41598-023-27528-0.